I-75 BRIDGE OVER SEXTON/KILFOIL DRAIN, THE LONGEST HIGHWAY BRIDGE SPAN PRESTRESSED WITH CFRP STRANDS

N. Grace [1], M. Chynoweth [2], T. Enomoto [3] and M. Bebawy [4]
[1] *Lawrence Tech. University, Southfield, MI, U.S.A., Email: ngrace@ltu.edu*
[2] *Michigan Dept. of Transportation, Lansing, MI, U.S.A.*
[3] *Tokyo Rope USA Inc., Canton, MI, U.S.A.*
Lawrence Tech. University, Southfield, MI, U.S.A.

ABSTRACT

Extensive experimental, analytical, and numerical research efforts resulted in the design and construction of the world longest highway bridge span prestressed with carbon fiber reinforced polymer (CFRP) strands. This 137-ft (41.8-m) long simply-supported bulb-T beam bridge carries I-75 highway over Sexton/Kilfoil Drain in Allen Park, Michigan, U.S.A. The bridge superstructure is composed of ten 72-in. (1.83-m) deep precast prestressed bulb T beams supporting a 9-in. (230 mm) thick cast-in-place reinforced concrete deck slab. One exterior beam is prestressed with a total of 69 CFRP strands due to the weight of an additional sound barrier wall, while the rest of the beams are prestressed with a total of 63 strands each. Each strand is tensioned with an initial prestressing force of 35 kip (156 kN), which represents approximately 65 % of the strand guaranteed strength after it is reduced with the appropriate environmental reduction factor. To ensure the safety and adequacy of the bridge to carry the assigned traffic loads and withstand the severe weather in Michigan, the design of the bridge underwent multiple revisions and test results from a parallel experimental investigation were utilized to make key design decisions. In addition, a finite element study was executed to evaluate the response of the bridge under different loads and environmental conditions. Furthermore, after bridge construction and before it was opened for traffic, a field load test using two standard trucks positioned at strategic locations on the bridge was executed. The strain and deflection values of three beams due to the truck loads were captured using onboard sensors. Field data were analysed and compared with finite element results and theoretical models to ensure adequate bridge performance.

KEYWORDS

Highway bridge, Prestressing CFRP, Field test, Bridge Design.

INTRODUCTION

Michigan Department of Transportation (MDOT) pioneers in the deployment of innovative materials such as non-corrosive CFRP to enhance the design, construction, and durability of highway bridge beams. This is partly motivated by the harsh Michigan weather and the overwhelming corrosion and durability issues associated with steel prestressed beam bridges. The use of CFRP as prestressing and reinforcement material started in Michigan in 2001 with the construction of Bridge Street bridge in Southfield, MI. Since then, several bridges have been successfully designed and constructed with CFRP components. For instance, in 2011, a two-span side-by-side precast prestressed box-beam bridge was constructed to carry Pembroke Rd over M-39 in Detroit, MI. The bridge is transversely post-tensioned with twelve 1.57-in. (40-mm) diameter un-bonded carbon fiber composite cable (CFCC) strands. In 2012, a three-span side-by-side box beam bridge carrying M-50 over NSRR railroad in Jackson, MI was also constructed and transversely post-tensioned using twenty un-bonded CFCC strands. In 2013 and 2014, two simply-supported 45°-skewed precast prestressed spread box-beam bridges were constructed to carry the east and west bounds of M-102 over Plum Creek in Southfield, MI. The box-beams are prestressed with 0.6-in. (15.2-mm) diameter CFCC strands and are provided with CFCC stirrups in the transverse direction. The cast-in-place deck slabs for both bridges are also reinforced with CFCC strands. In 2016, a 102.5-ft (31.2-m) long simply-supported bulb T-beam bridge was constructed to carry M-86 over Prairie River in Centreville, MI. Each of its seven bridge beams is prestressed with 59 CFCC strands with a diameter of 0.6 in. (15.2 mm). The latest and longest completed bridge project (Oct 2017) with CFRP reinforcement is carrying I-75 highway over Sexton and Kilfoil Drain in Allen Park, MI. This single span simply-supported bridge has an effective span of 137 ft (41.8 m) and a deck width of 63.3 ft (19.3 m) with a clear roadway of 60 ft (18.3 m). The bridge is composed of ten bulb T beams supporting a 9.0 in. (230-mm) thick cast-in-place reinforced deck slab. Before the bridge was opened for traffic, a field load test was executed by placing two 55-kip (245-kN) trucks at key locations near the mid-span and recording the response of the bridge using onboard sensors. The response of the bridge was compared with that expected theoretically and with the results from a finite element model. This manuscript documents some of I-75 bridge design and construction issues and provides the results of field load test.

I-75 BRIDGE OVER SEXTON/KILFOIL DRAIN

Design

Mechanical and physical properties of CFRP affect some design aspects of CFRP prestressed beams. For instance, jacking and prestress level is limited by the one-million-hour creep rupture strength of CFRP. Currently ACI 440.4R-04 limits the jacking stress to 65 % of the guaranteed strength although recent studies suggest much higher creep rupture strength. In addition, the coefficient of thermal expansion of CFRP is nearly negligible compared to that of concrete. Therefore, CFRP prestressed beams experience increase or decrease in the effective prestressing force with the increase or decrease in temperature, respectively. This kind of thermal gain or loss in prestressing force shall be considered when establishing the initial prestressing force. Other types of prestress loss such as elastic prestress loss and long-term loss due to concrete creep and shrinkage do not seem to be affected by the properties of the reinforcement and can be calculated using conventional equations and approximate methods developed for steel prestressed beams.

Once the prestressing force level is established, the analysis of a CFRP prestressed section becomes a straightforward process with few exceptions. For instance, steel reinforced/prestressed sections are classified as tension-controlled or compression-controlled according to the net tensile steel strain at the time the concrete in compression reaches its assumed crushing strain limit of 0.003. However, CFRP reinforced/prestressed sections are classified as tension or compression-controlled based on the actual failure mode whether it is crushing of the concrete or rupture of the CFRP reinforcement. If the concrete reaches a crushing strain of 0.003 while the net strain in the extreme CFRP remains less than net guaranteed tensile strain, the section is regarded as compression-controlled section. If the net extreme CFRP strain reaches the net guaranteed tensile strain, while the concrete compression strain remains less than 0.003, the section is regarded as tension-controlled. The net guaranteed tensile strain is the net tensile strain in the reinforcement at balanced strain conditions. For all prestressed CFRP reinforcement, the net guaranteed strain limit may be taken as the specified guaranteed ultimate strain exclusive of the strain due to prestress, creep, shrinkage, and temperature.

Whether the section is compression-controlled or tension-controlled, the nominal moment capacity can be calculated using the principles of strain compatibility and force equilibrium in the section. ACI 440.4R-04 provides equations to calculate the depth of the neutral axis and nominal moment capacity of the section when the reinforcement or prestressing CFRP are provided in a single layer. Nevertheless, due to the elastic nature of CFRP material, when the tension CFRP reinforcement is distributed over multiple layers, the failure of tension-controlled sections is usually governed by the failure of CFRP reinforcement at the extreme layer, which is the layer farthest from the compression fiber. CFRP reinforcements at layers closer to the compression fiber are likely to fail progressively once CFRP reinforcement at the extreme layer fails. It is therefore not recommended to sum the layers of CFRP reinforcements through their center of gravity. ACI 440.4R-04 Section 3.4.2 provides a set of equations to address this problem. Nevertheless, the equations in ACI 440 are based on the assumption that the stress distribution in concrete is linear and the section is tension-controlled and therefore, those equations are not applicable for compression-controlled sections or tension-controlled section with non-linear stress distribution on the concrete. That leaves the designer with the option of using basic strain compatibility and force equilibrium. However, strain compatibility and force equilibrium in their raw format tend to be a lengthy iterative process, especially when the mode of failure is not known.

To facilitate the flexural design and reduce the potential for error, a unified design approach is developed by converting the areas of CFRP reinforcement at different layers to equivalent areas at the level of the extreme CFRP layer using appropriate area reduction factors. The sum of equivalent reinforcement areas at the extreme layer is regarded as "The equivalent area of reinforcement, A_{fe}" and is used to calculate the depth of the neutral axis and the nominal moment capacity of the section. In other words, the equivalent area of CFRP reinforcement is a discrete area of CFRP reinforcement positioned at the extreme CFRP layer that results in the same flexural capacity of n layers of reinforcement.

The area reduction factors needed to calculate the equivalent areas of reinforcement are obtained by assuming linear strain distribution through the depth of the section. Thereby, the area of CFRP reinforcement at the ith layer is reduced with a factor depending on the distance from the ith layer to the extreme layer. The area reduction factor can be calculated by evaluating the strain distribution through the section as follows:
The net tensile strain at any layer (i) is related to the net tensile strain at the extreme CFRP layer by:

$$\varepsilon_i = \varepsilon_1 \left(\frac{d_i - c}{d_1 - c} \right) \quad (1)$$

where:

ε_i = net tensile strain at the *ith* CFRP reinforcement layer
ε_1 = net tensile strain at the extreme CFRP layer
d_i = depth of the *ith* CFRP layer from the extreme compression fiber (in. or mm)
d_1 = depth of the extreme CFRP layer from the extreme compression fiber (in. or mm)
c = depth of neutral axis from the extreme compression fiber (in. or mm)

The tensile force, T_i, in any CFRP layer (i) may be calculated as:

$$T_i = \varepsilon_i N_i a_f E_f = \varepsilon_1 \left(\frac{d_i - c}{d_1 - c}\right) N_i a_f E_f = \varepsilon_1 \left(\frac{d_i - c}{d_1 - c} N_i a_f\right) E_f = \varepsilon_1 A_{fe(i)} E_f \quad (2)$$

where:
ε_i = net tensile strain at the *ith* CFRP reinforcement layer
N_i = number of CFRP strands in the *ith* layer
a_f = area of single CFRP strand in the *ith* layer (in.^{2} or mm^2)
E_f = elastic modulus of CFRP (ksi or MPa)
d_i = depth of the *ith* CFRP layer from the extreme compression fiber (in. or mm)
d_1 = depth of the extreme CFRP layer from the extreme compression fiber (in. or mm)
c = depth of neutral axis from extreme compression fiber (in. or mm)

where $A_{fe(i)}$ is the area equivalent to the area of CFRP reinforcement at layer i and is calculated as:

$$A_{fe(i)} = \frac{d_i - c}{d_1 - c}(N_i a_f) \quad (3)$$

The equivalent area of reinforcement for the total reinforcement provided in the section, A_{fe} is calculated as:

$$A_{fe} = \sum_{i=1}^{n} A_{fe(i)} \quad (4)$$

Where
n = number of layers (rows) of CFRP reinforcement

At this stage of analysis, the depth of the neutral axis from the extreme compression fiber, c, can be initially set equal to $0.1d_1$. The initial assumption of $c = 0.1d_1$ is based on observations from multiple experimental flexural tests of CFRP prestressed beams. This assumption usually yields accurate estimate for the depth of the neutral axis and the flexural capacity of the section. It needs not to be adjusted unless more refined calculations are required. With $c = 0.1d_1$, Eq. 3 becomes:

$$A_{fe(i)} = \left(1 - \frac{s_i}{0.9d_1}\right)(N_i a_f) \quad (5)$$

where:
s_i = Distance between *ith* CFRP layer and extreme CFRP layer (in.) = $d_1 - d_i$

After establishing the equivalent area of reinforcement for the section, the exact depth of neutral axis shall be calculated from Eqs. 6 through 9, whichever is applicable:

For tension-controlled flanged sections:

$$c = \frac{E_f A_{fe}\left(\varepsilon_{gu} - \varepsilon_{pe}\right) + P_e - 0.85 f_c' h_f (b - b_w)}{0.85 f_c' \beta_1 b_w} \quad (6)$$

For tension-controlled rectangular sections:

$$c = \frac{E_f A_{fe}\left(\varepsilon_{gu} - \varepsilon_{pe}\right) + P_e}{0.85 f_c' \beta_1 b} \quad (7)$$

For compression controlled flanged sections:

$$0.85\, f_c'\, \beta_1\, b_w\, c + 0.85\, f_c'\, h_f\, (b - b_w) = E_f\, A_{fe}\, \varepsilon_{cu} \left(\frac{d_1}{c} - 1\right) + P_e \quad (8)$$

For compression-controlled rectangular sections:

$$0.85\, f_c'\, \beta_1\, b\, c = E_f\, A_{fe}\, \varepsilon_{cu} \left(\frac{d_1}{c} - 1\right) + P_e \quad (9)$$

where:

b = width of compression face of the member; for a flanged section in compression, the effective width of the flange (in. or mm)
P_e = effective prestressing force in the section (kip or N)
E_f = elastic modulus of CFRP (ksi or MPa)
ε_{cu} = average concrete crushing strain, 0.003
ε_{gu} = design guaranteed strain of CFRP including environmental and durability effects
ε_{pe} = effective prestressing strain in CFRP after subtracting applicable prestress losses
h_f = depth of compression flange (in. or mm)
b_w = width of web (in. or mm)

Equation 6 through 9 are developed by representing the natural relationship between concrete stress and strain by an equivalent rectangular concrete compressive stress block of $0.85f_c'$ over a zone bounded by the edges of the cross-section and a straight line located parallel to the neutral axis at the distance $a = \beta_1 c$ from the extreme compression fiber. The distance c is measured perpendicular to the neutral axis. The factor β_1 is taken as 0.85 for concrete strengths not exceeding 4.0 ksi (28 MPa). For concrete strengths exceeding 4.0 ksi (28 MPa), β_1 is reduced at a rate of 0.05 for each 1.0 ksi (6.89 MPa) of strength in excess of 4.0 ksi (28 MPa), except that β_1 shall not be taken to be less than 0.65.

After calculating the depth of the neutral axis, the nominal moment capacity of the section can be calculated for flanged sections subjected to flexure about one axis and where the compression flange depth is less than $a = \beta_1 c$ as follows:

$$M_n = \sum_{i=1}^{n} \left[a_f\, N_i\, \varepsilon_i\, E_f \left(d_i - \frac{a}{2}\right)\right] + P_e \left(d_p - \frac{a}{2}\right) + 0.85\, f_c'\, h_f\, (b - b_w) \left(\frac{a}{2} - \frac{h_f}{2}\right) \quad (10)$$

where:

a_f = area of single CFRP strand in the ith layer (in.2 or mm2)
N_i = number of CFRP strands in the ith layer
ε_i = net tensile strain at the ith layer of CFRP reinforcement determined from strain compatibility, taken equal to $\varepsilon_1 \left(\frac{d_i - c}{d_1 - c}\right)$
ε_1 = net tensile strain at the extreme CFRP layer
d_i = depth of the ith CFRP layer from the extreme compression fiber (in. or mm)
d_1 = depth of the extreme CFRP layer from the extreme compression fiber (in. or mm)
f_c' = specified compressive strength of concrete at 28 days, unless another age is specified (ksi or MPa)
P_e = effective prestressing force in the section (kip or N)
d_p = distance from the extreme compression fiber to the centroid of prestressing strands (in. or mm)
E_f = elastic modulus of CFRP (ksi or MPa)
h_f = depth of compression flange (in. or mm)
b = width of compression face of the member (in. or mm)
b_w = width of web (in. or mm)
a = $\beta_1 c$; depth of the equivalent stress block (in. or mm)
β_1 = stress block factor
c = depth of neutral axis from extreme compression fiber as determined from Eqs. 6 through 9, whichever is applicable (in. or mm)
n = number of layers (rows) of CFRP reinforcement

For rectangular sections subjected to flexure about one axis, where the approximate stress distribution is used and where the compression flange depth is not less than $a = \beta_1 c$ as determined in accordance with Eqs. 6 through 9, whichever is applicable, the nominal flexural resistance M_n may be determined by using Eq. 10, in which case b_w shall be taken as b.

For I-75 bridge, all beams except one exterior beams were prestressed with a total of 63 CFCC strands with a diameter of 0.6 in. (15.2 mm), cross sectional area of 0.179 in.^{2} (115.4 mm^2), guaranteed tensile strength of 339 ksi (2.34 GPa), and elastic modulus of 21,000 ksi (147 GPa). Due to a significant dead load on the exterior beam, the number of CFCC strands increased to 69 strands for this beam only. All strands are prestressed with an initial prestressing force of 35 kip (156 kN) per strand. Figure 1 shows the cross section and prestressing layout in the beams. The transverse reinforcement, top flange reinforcement and deck reinforcement were made of epoxy coated steel reinforcing bars. During design, the Service Limit State was the governing state in establishing the number of strands based on the required level of prestressing force. The beams were designed to have no tension in the bottom flange under Service Limit State. Nominal moment capacity was calculated according to the equivalent area method and the results were verified by force equilibrium and strain compatibility of the section. Loads and distribution factors of bridge beams conformed to AASTHO LRFD (2014) design specifications. In addition, the bridge is provided with a single steel diaphragm at the mid-span as shown in Figure 1 and cast-in-place concrete diaphragms at the ends that were poured with the deck slab.

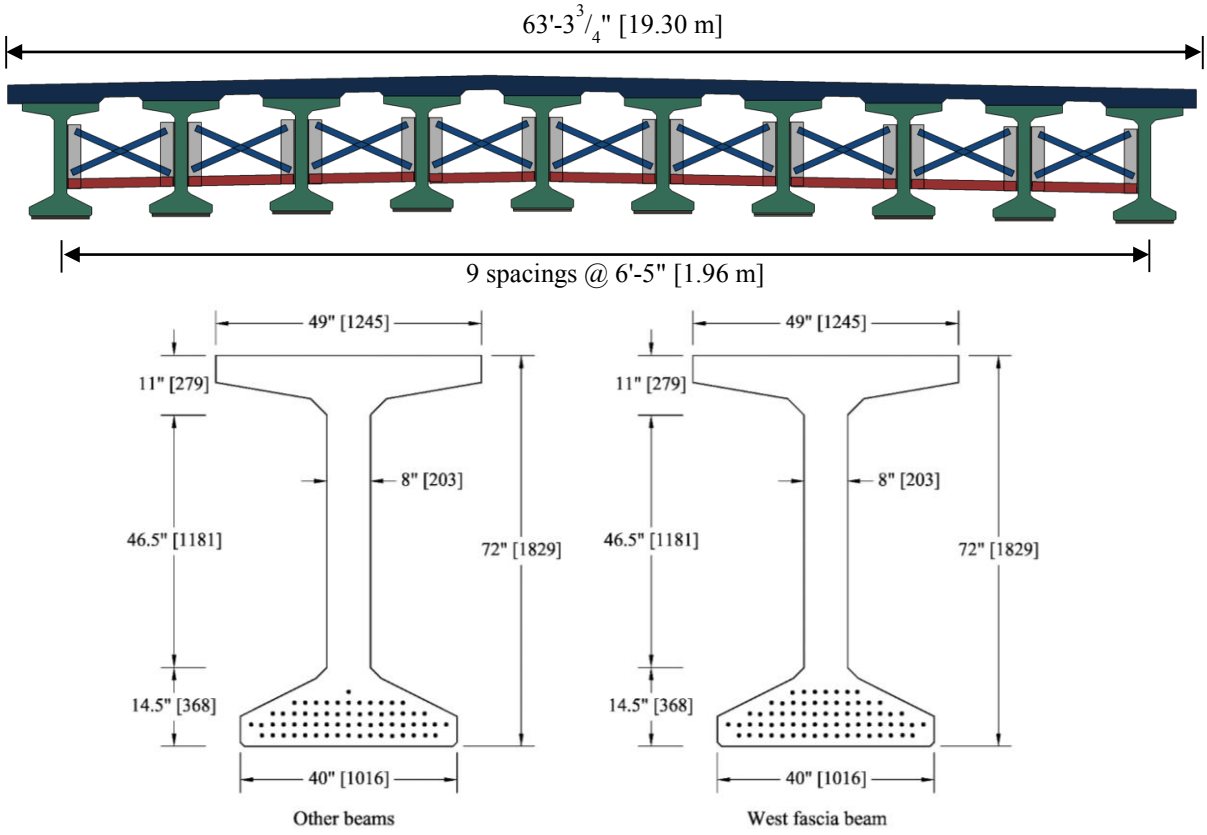

Figure 1: Cross section and distribution of prestressing CFCC strands in bridge beams

Finite Element Analysis (FEA) and Bridge Construction

Prior to beam construction, three finite element models were generated to simulate different stages of bridge construction and loading. The first model represented a single beam without a deck slab at the precaster plant. The beam model was analysed under initial prestressing force and the self-weight to evaluate the stresses and the camber in the beam at the time prestress release and during shipping and handling. The second finite element model represented a single beam with a deck slab. The model was analysed under construction and dead loads and an incremental live load represented by a two-point-load at the mid-span (four-point-loading setup). The live load was increased gradually until the failure of the beam model and consequently the numerical nominal moment capacity of the beam was determined. The third model simulated the full bridge and was analysed under effective prestressing force, dead loads, superimposed dead loads, wind loads, and traffic loads represented by a vehicular loading HL-93 according to AASHTO LRFD (2014) accompanied by extreme environmental conditions such as hot and cold weathers.

After verifying all design criteria using the FEA, construction of the beams was approved. The beams had a length of 138.33 ft (42.16 m) and were constructed in an abutment-type prestressing bed. To facilitate beam construction, CFCC strands were coupled with low-relaxation steel strands at both ends using a special coupler system. This enabled construction crew to execute the prestressing using conventional hardware that is used for steel. Prestress

loss due to change in temperature from the time of prestressing to the time of pouring the concrete was estimated and considered in the jacking force. Due to concerns with high tensile stresses at beam ends during shipping and handling, the beams were constructed using a concrete mix with a design 28-day compressive strength of 10 ksi (69 MPa) and strength at release of 8 ksi (55 MPa). Figure 2 document different stages of beam and bridge construction.

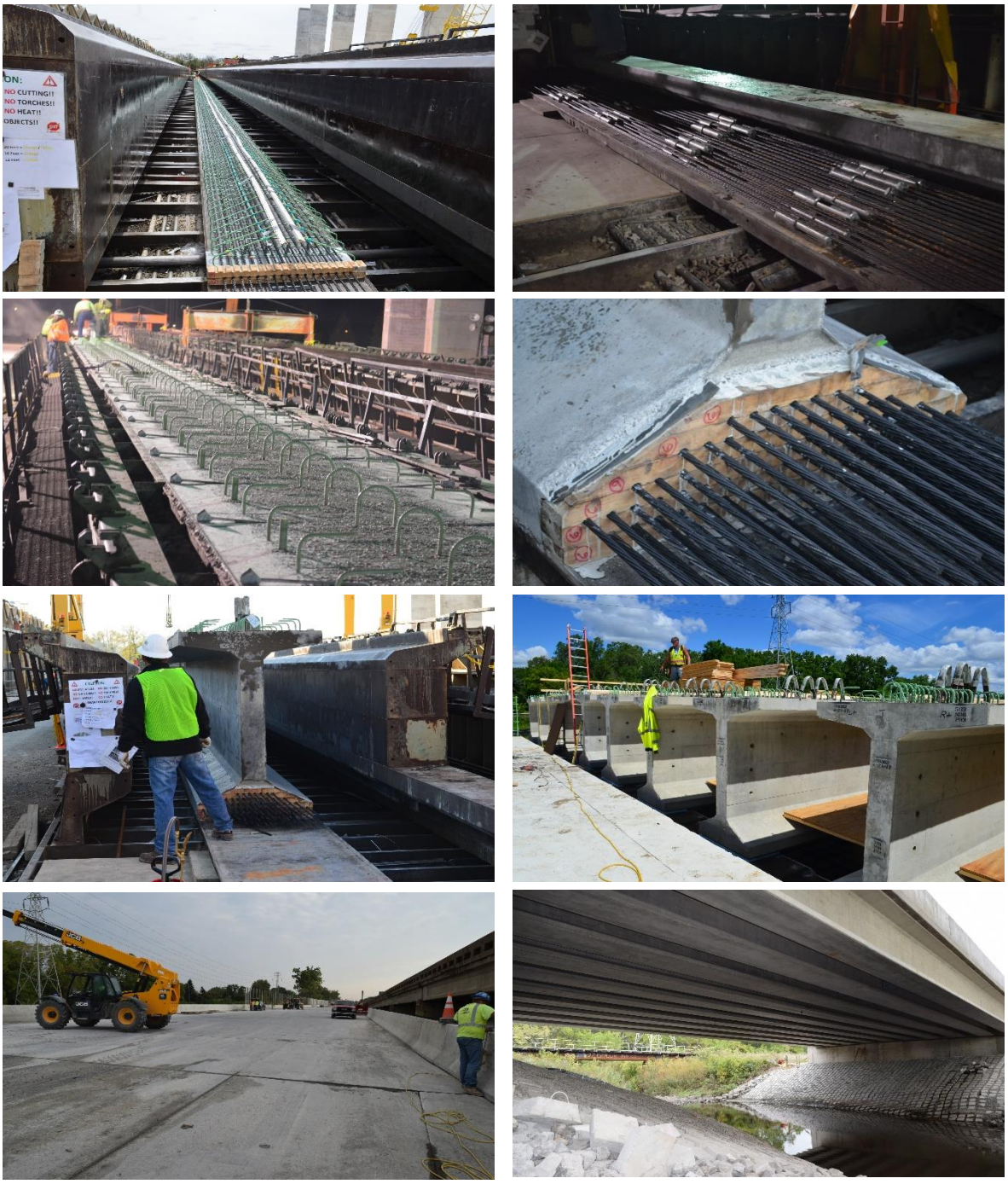

Figure 2: Construction of I-75 bridge over Sexton/Kilfoil Drain

Field Load Test

After completing the bridge construction and before it was opened for traffic, a field load test was executed to evaluate the bridge response and verify the design parameters. Two loaded 7600 international trucks, weighing approximately 55 kip (245 kN) each, were used to execute the load test. The clear bridge width of 60 ft (18.3 m) was divided into five 12-ft (3.7-m) wide lanes and the two trucked were positioned at seven locations as shown in Figure 3 near the bridge mid-span. The last location included placing the two trucks back-to-back (BTB) at the

first lane near the exterior beam. Readings from strain gages attached to three beams were collected. In addition, the deflection of the beams was captured using a total station. Furthermore, the finite element model was analysed under the weight of the field trucks at the seven different locations. The stress, strain, and deflection due to truck loads at each location were estimated from the FEA and plotted against the anticipated theoretical values and the measured values from the field.

I: One truck on Lane 1

II: Two trucks on Lanes 1 & 2

III: Two trucks on Lanes 2 & 3

IV: Two trucks on Lanes 3 & 4

V: Two trucks on Lanes 4 & 5

VI: One truck on Lane 5

VII: Two back-to-back trucks on Lane 1

Figure 3: Seven truck locations during field load test using two 7600 international trucks

RESULTS AND DISCUSSIONS

As shown in the figures 4 and 5, there is a good agreement between the field strain readings and the finite element model. In addition, the deflection readings agreed well with those from the FEA. Furthermore, the reserve capacity of the bridge was determined by estimating the strain due to the design HL-93 vehicular loading and comparing the values with those obtained from the field test.

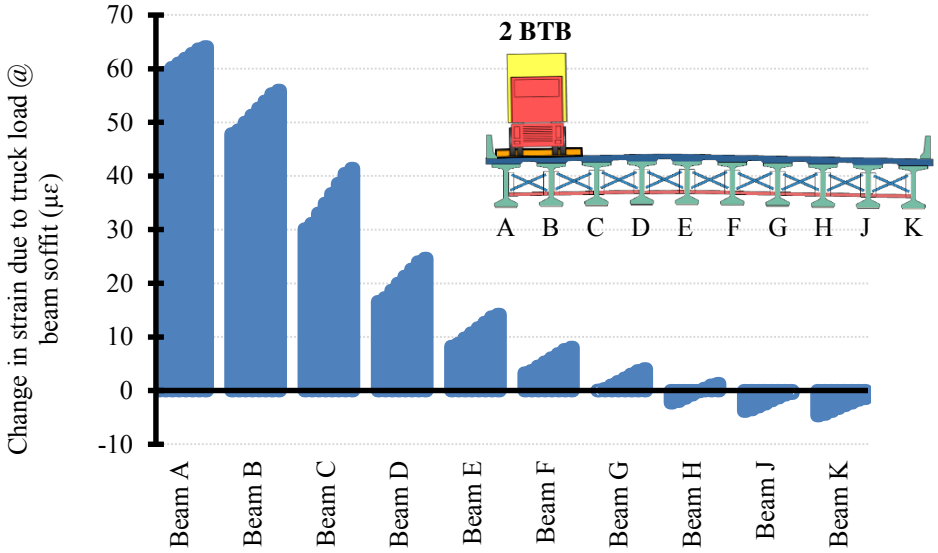

Figure 4: Change in strain in bridge beams due to two back-to-back field trucks (FEA)

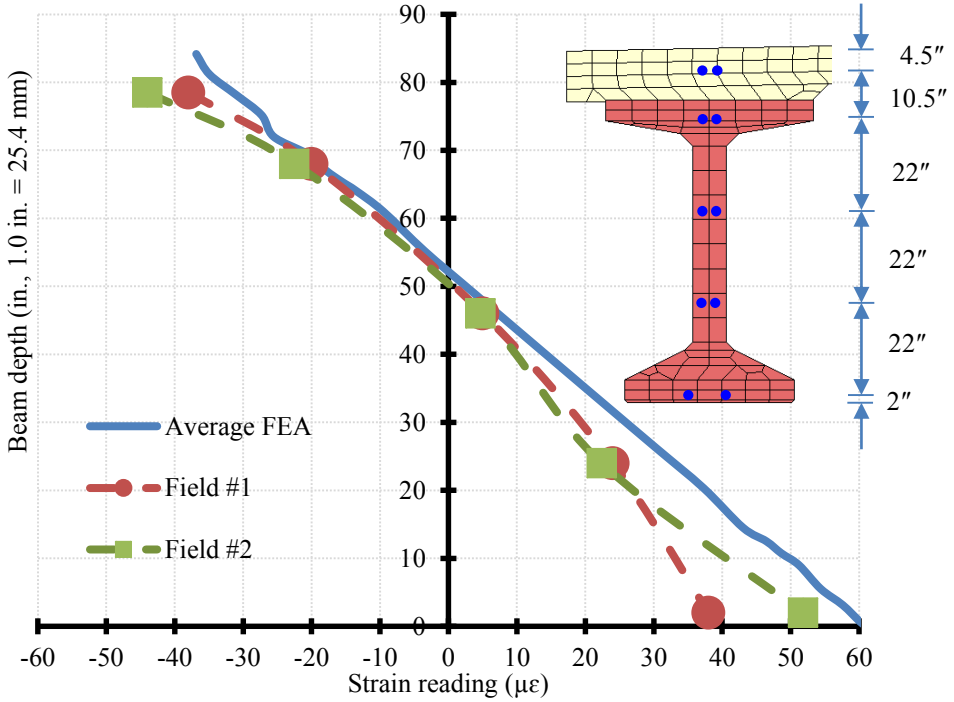

Figure 5: FEA and measured strain readings in Beam A due to two back-to-back field trucks @ lane 1

CONCLUSIONS

Results from the field load test verified the adequacy of the design procedure and the results of the finite element study. They also provided confidence in the CFRP material and the full bridge to support traffic loads. Therefore, it can be concluded that design and construction of highway bridges with CFRP reinforcement is a promising technique to mitigate the corrosion problem. With the appropriate design philosophy and the proper handling for the CFRP material, the design and construction can be a straightforward process.

REFERENCES

ACI Committee 440 (2004). “Prestressing Concrete Structures with FRP Tendons”, P35, American Concrete Institute (ACI), Farmington Hills, MI.

American Association of State Highway and Transportation Officials (AASHTO) Committee (2014). "AASHTO LRFD Bridge Design Specifications, 7th edition", Washington, DC.